Thin Solid Films, 205 (1991) 176–181

Dynamic fracture test of metal thin films deposited on an insulating substrate by a high current pulse method

Kwang Yul Kim and Wolfgang Sachse

Department of Theoretical and Applied Mechanics, Thurston Hall, Cornell University, Ithaca, NY 14853 (U.S.A.)

(Received February 5, 1991; accepted May 21, 1991)

Abstract

In this paper we describe a novel technique for determining the dynamic fracture strength of metal thin films deposited on an insulating substrate by flowing through the films a high current pulse of short duration. Examples are provided with the films of high conductivity materials such as aluminum, copper, gold and silver, which were all deposited on a fused quartz disk. The high current flow heats the film, which is then loaded with thermal stresses caused by a mismatch of thermal expansions of the film and substrate materials. On heating, the thin film is subjected to a state of triaxial compression.

Among the film materials tested, copper shows the toughest fracture strength and gold the weakest. The fracture strengths of silver and aluminum films lie between those of the gold and copper films.

1. Introduction

Characterization of mechanical properties of thin films deposited on a substrate has become increasingly important in improving the quality and performance of thin films which have found innumerable applications in semiconductor industries, for extension of tool lifetime, and also for protective anticorrosion coatings, among others. The great bulk of the work in this area has been devoted to characterizing the adhesion strength measured in the direction normal to the plane of films lying on the surface of the substrate and has been summarized by Mittal [1,2]. While the adhesion strength of the film obtained in the direction normal to the film plane is very important for characterization and improvement of adhesion of the thin films, little work has been published in characterizing the mechanical properties of thin films subjected to biaxial or triaxial stresses, which may repeatedly arise, for instance, as a result of Joule heating induced by the frequent switch-on and continuous-on of an electrical current flow. Depending on the configuration of the thin film devices, the film is more likely to be under these biaxial or triaxial thermal stresses than under a uniaxial normal stress which is directly related to the adhesion of the films. The thermal stresses acting on the film as a result of the current flow are caused by a mismatch of the thermal expansions of the film and substrate materials. Repeated switch-on and -off of the thin film devices will progressively weaken the films, which will ultimately lead to failure by fatigue fracture.

We have recently reported preliminary results [3,4] on the determination of the fracture strength of thin films of silver adhered on a plate of soda–lime glass. However, the focus of this work was on the characterization of the source of acoustic emission of a thin film which also acted as a source of thermoelastic waves that propagated through the substrate medium. Our present work is basically the extension and refinement of our previous work, but devoted to the characterization of fracture of thin films. Here we present a novel technique for the determination of dynamic fracture strength of metal thin films deposited on a fused quartz disk by a sputtering technique. Materials chosen for the thin film fracture test are high conductivity metals including aluminum, copper, gold and silver.

2. Experimental set-up

A detailed description of the experimental set-up for the fracture test of thin films is essentially the same as that given in refs. 3 and 4, and its block diagram is shown in Fig. 1. The high current pulse generator was capable of delivering a maximum current of about 100 A over a 100 μs time interval with a maximum voltage limit of about 950 V across the specimen. It also generates variable duration, high current pulses of different frequencies to about 1 MHz. The magnitude and duty cycle of these pulses were limited by the stored energy of the instrument in excess of 400 J. The rise and fall times of the high current pulses were respectively less than 20 ns and 50 ns. The insulating substrate was a 75 mm square fused quartz

0040-6090/91/$3.50

disk on which several parallel strips (not shown in Fig. 1) of thin films, about 50 mm long and 1.59 mm wide, were deposited by using a sputtering technique. The thicknesses of all the thin films tested were less than 1 μm. The bottom side of two small brass plates that faced the film strip was bonded with a 0.15 mm thick gold foil by using a silver–epoxy cement and was pressed onto the thin film strip during the test. The gold foil minimized the cold contact resistance which might cause problems during the sudden application of a high current pulse. The distance between two brass–gold plates was maintained at 32.4 mm. Each brass–gold plate had two electrodes. One electrode was used for the current flow and the other for the potential measurement.

A high current pulse with magnitude ranging from about 1 to 100 A and a duration of about 100 μs was fed from the generator to the thin films. The magnitude of the current flowing through the film was measured by a current probe which had a sensitivity of 0.1 V A^{-1} with a bandwidth extending from 1 Hz to 20 MHz. The output of the current probe and the voltage across the film were both digitized in a two-channel waveform recorder that operated at a 10 MHz sampling rate with a 10-bit resolution. Because of the varying magnitude of the voltage across the film, which extended from less than 1 V to close to 1000 V, a variable attenuator was used to bring the attenuated thin film voltage into the digitizer as shown in the figure. The generation of the current pulse and digitization of the signals were synchronized by using the trigger pulse derived from the voltage pulse–function generator. Recorded signals in the digitizer were visually displayed on an x–y scope and transferred into an interactive microcomputer-based data acquisition system for data storage and subsequent data analysis.

Throughout the experiment a single current pulse of monostable mode with a duration of about 100 μs was applied to every specimen for fracture testing of the film. During the application of the high current pulse both temperature and electrical resistance of the film increased. As a result, the voltage across the film increased monotonically with time, building up enough thermal stresses that could eventually cause the film to fracture. It was experimentally found that repeated applications of the same magnitude current pulse or a gradually increasing pulse in magnitude significantly reduced the fracture strength of the thin film because of fatigue. If the current pulses were not applied systematically, the reduced fracture strength was observed to have a large variation. Since a study of fatigue fracture is left for future work and not within the scope of the present study, only a single-shot current pulse with magnitude well above the level that can cause the film to fracture with certainty during its duration was applied once to every specimen to avoid fatiguing the film. This current level depends on the film material and was easily found by testing two or three

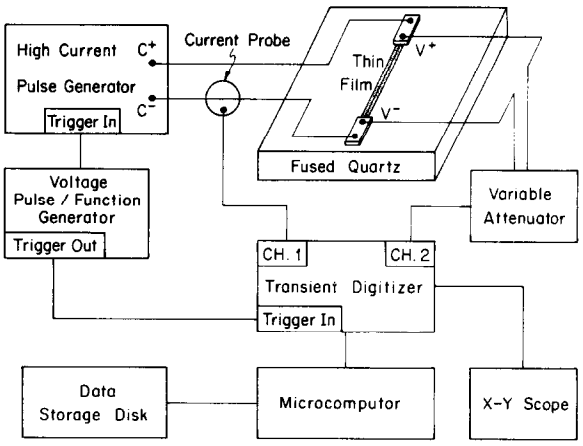

Fig. 1. An electronic block diagram of the experimental set-up.

specimens to which gradually increasing current pulses were applied until they fractured. This way, fairly consistent fracture strengths were obtained for the films of the same material. These fracture strengths were also found to vary very little with the magnitude of the single current pulse, although current pulses with different magnitudes induced various loading rates of thermal stresses on the film. This situation may be analogously compared with a mechanical Charpy V-notch impact test which is used to determine the dynamic fracture strength of materials. Therefore, the magnitude of the current pulse was rather arbitrarily set well above the fracture-inducing level and remained unchanged for the films of the same material. During application of the pulse more than one fracture was usually observed at different locations in the film, causing sharp changes in the voltage across the film at the instants when the film fractured. An optical micrograph of a fractured gold film is shown in Fig. 2. It appeared that, once fracture initiated through

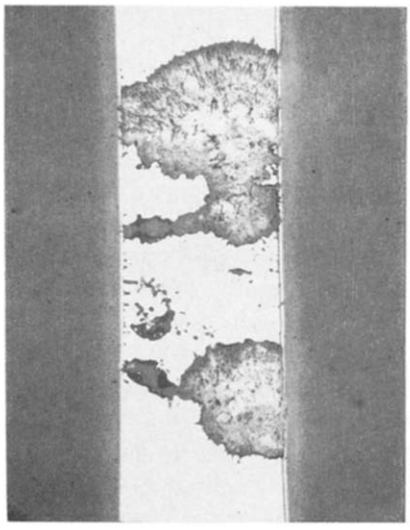

Fig. 2. An optical micrograph of the fractured gold film. The white band in the middle is the fractured gold film with width 1.59 mm.

the film, there occurred a high concentration of current density and thermal stresses at the crack tip and therefore the crack front melted away rapidly, propagating very fast and leaving the exposed substrate behind.

3. Theory

The temperature of a metal thin film, heated by the resistance to the flow of a high current pulse with magnitude I, rises and likewise the electrical resistance R of the film increases. This temperature of the thin film is assumed to be uniform throughout the volume between the two brass–gold plates. This may well be justified because of the very high thermal conductivities of the thin film materials and a very low thermal diffusivity of the substrate material, a very thin film thickness, and the short duration of the applied current pulse. Denoting the initial resistance of the film and the temperature coefficient of the unit resistance as R_0 and γ respectively, the electrical resistance R of the film can be expressed as

$$R(t) = R_0\{1+\gamma\theta_f(t)\} \tag{1}$$

where θ_f is the temperature rise of the film and t represents time. Then the potential drop E across the film is

$$E(t) = I(t)R(t) = I(t)R_0\{1+\gamma\theta_f(t)\} \tag{2}$$

Both $I(t)$ and $E(t)$ in eqn. (2) are determined experimentally and $R(t)$ can be obtained by dividing $E(t)$ by $I(t)$. The temperature rise $\theta_f(t)$ of the film can be calculated from eqn. (1) with knowledge of R_0 and γ. It has been reported [5] that the electrical resistivity is independent of the film thickness except for the extremely thin films whose thickness approaches the electronic mean free path. Therefore, the value of γ corresponding to the bulk material has been used for the thin films for eqns. (1) and (2).

The heated metal film will freely expand in the absence of a substrate. However, when the film is attached to a substrate, thermal expansion of the film is constrained by the film–substrate interface and therefore stressed by a mismatch between their thermal expansions. This thermoelastic problem was previously analysed by Aleck [6] and further refined by Blech and Levi [7]. The thermoelastic forces acting on the edges of the thin film are easy to visualize and schematically displayed in Fig. 3 which also shows the reference coordinate system used for the calculation of thermal stresses. The origin of the reference system is at the middle of the top surface of the film. Let E_f, ν_f, and α_f denote respectively the Young's modulus, Poisson's ratio, and linear thermal expansion coefficients of the film and let α_s be the linear thermal expansion coefficient of the substrate. According to refs. 6 and 7, except in the region very close both to the film edges and to the brass–gold plates, thermal stresses acting everywhere on the film are

$$\sigma_{xx} = \sigma_{yy} = \frac{E_f}{1-\nu_f}(\alpha_s-\alpha_f)\theta_f \tag{3}$$

$$\sigma_{zz} = \sigma_{xy} = \sigma_{xz} = \sigma_{yz} = 0 \tag{4}$$

Since the length and width of the film are much larger than the film thickness and $\alpha_f \gg \alpha_s$, the thin film is subjected to two equal biaxial compressive stresses everywhere except very close to the film edges. Within a distance of a few film thicknesses from the film edge, the spatial distribution of σ_{zz} and the shear stresses exhibit a complex pattern (see ref. 7), while both σ_{xx} and σ_{yy} rapidly converge to zero as one approaches the edge of the film. Fortunately, we are not concerned with the stresses acting very near or at the film edge, since all the film fractures were experimentally observed to initiate in the region far away from the edge of the film and from the boundary of the film and brass–gold plate, as compared with the film thickness. This may be in part attributed to the fact that temperatures in the region very near the film edges and very close to those boundaries, because of more effective heat losses, are somewhat lower than the uniform temperature in the interior region of the great bulk of the film. Consequently, we have only to deal with the two equal compressive stresses given by eqn. (3). The orientations of fracture-induced cracks were observed to be random in general as expected from two-dimensional hydrostatic compression acting only in the plane of the thin film.

Dynamic fracture of the film, once initiated, propagated in a seemingly brittle manner and often

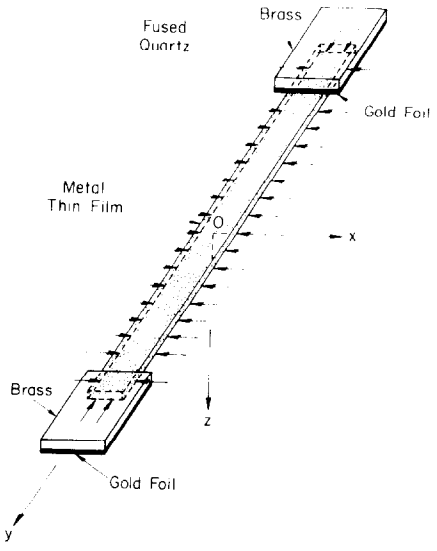

Fig. 3. A schematic diagram which shows thermoelastic forces acting on the thin film and the reference coordinate system.

catastrophically, contrary to the ductile fracture observed in bulk specimens of the same material under purely mechanical loading. The Griffith theory [8,9] developed for fracture in the uniaxial and biaxial stresses can be extended to fracture under triaxial stresses. It is desired to find a crack with the most critical orientation. It seems reasonable to assume that such a crack will have its plane parallel to the plane of the axis of intermediate principal stress, which can be in any direction in the x–y plane or the plane of the thin film, as can be seen in eqns. (3) and (4). This is consistent with the experimentally observed crack orientations. Since this intermediate stress plays no role in stress concentration, one can use the biaxial Griffith theory [9] developed for tension as well as compression. Two principal stresses under consideration are σ_{zz} and the stress acting normal to the crack orientation in the plane of the film. The latter stress is in magnitude equal to σ_{xx} or σ_{yy} given in eqn. (3). Then the Griffith criterion for fracture is

$$\sigma_{xx} = \sigma_0 \quad \text{if } 3\sigma_{xx}+\sigma_{zz}>0 \tag{5}$$

$$(\sigma_{xx}-\sigma_{zz})^2+8\sigma_0(\sigma_{xx}+\sigma_{zz}) = 0 \quad \text{if } 3\sigma_{xx}+\sigma_{zz}<0 \tag{6}$$

where $\sigma_0(\sigma_0>0)$ is the fracture stress under uniaxial tension. Since $\sigma_{zz} = 0$ and $\sigma_{xx}<0$ (compression), eqn. (6) holds as a fracture criterion for uniaxial compression. Fracture in the film takes place when

$$\sigma_f^* = \sigma_{xx}^* = \frac{E_f^*}{1-\nu_f^*}(\alpha_s^*-\alpha_f^*)\theta_f^* = -8\sigma_0^* \tag{7}$$

where the superscript * denotes the value taken at the fracture initiation temperature and σ_f^* is the corresponding thermal fracture stress acting in the plane of the film. Equation (7) is a well-known result. That is, the uniaxial compressive fracture strength of a brittle material is about eight times as much as its tensile strength.

4. Experimental data and results

Figures 4(a), 4(b) and 4(c) display a typical example of the current pulse applied through the film, the voltage across the film and the electrical resistance curve obtained by dividing the voltage by the current respectively. The figure was obtained with a gold film. Two sharp spikes observed in the individual curve correspond to two distinctive fracture events in the sample. Only the first fracture event was used in our analysis because it is very difficult to calculate film temperatures associated with subsequent cracks. The resistance at the initiation of the first crack was conveniently determined by differentiating a resistance curve with respect to time and taking a value at the point at which dR/dt suddenly changes. This is illustrated in Fig. 4(d). Also shown in Fig. 5 are typical resistance data measured with thin films of aluminum, copper, gold and silver. The initial portion in the resistance curve includes the transient effect caused by the system reactance, which was found to decay out 2 μs after the application of the pulse. The initial resistance R_0 was then obtained by extrapolating to the initial time of the pulse application from the curve determined through a least-squares goodness fit of the resistance data between 3 and 20 μs into a cubic polynomial. R_0 determined this way is found to be in good agreement with that measured statically using an ordinary digital multimeter. The extrapolated values of R_0 and R at the time of fracture initiation were used to calculate the temperature rise θ_f^*, according to eqn. (1), with a knowledge of γ found in the literature [10].

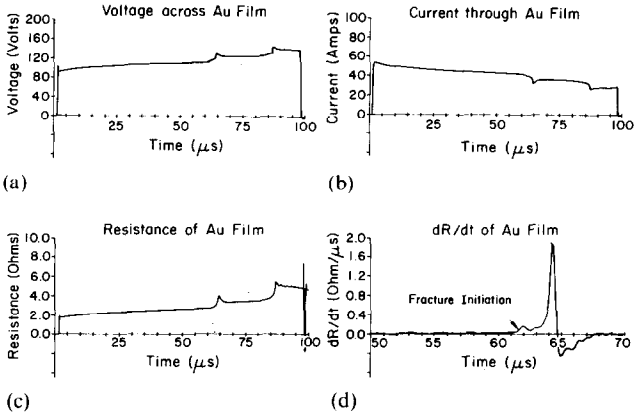

Fig. 4. Signals obtained with a gold film: (a) potential drop across the gold film; (b) current through the gold film; (c) resistance of the gold film; (d) differentiation of the resistance with respect to time around fracture initiation.

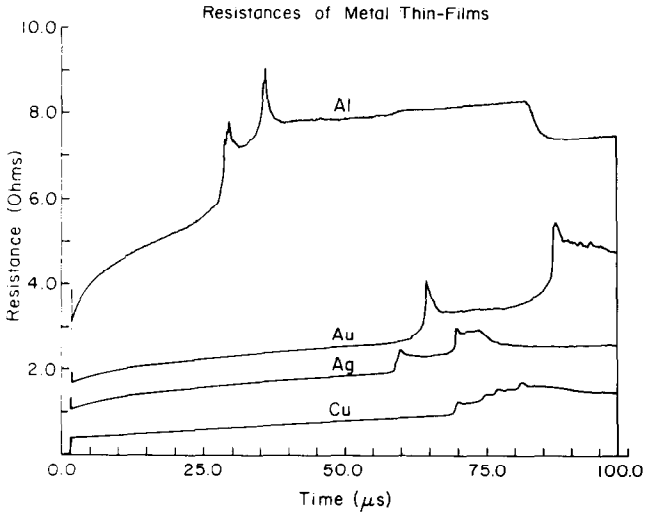

Fig. 5. Resistance data of aluminum, copper, gold and silver thin films.

Polycrystalline thin films are known to exhibit some degree of anisotropy as a result of texture introduced during a deposition process. This anisotropy is very difficult to access in the evaluation of elastic moduli and

would probably not be large, as it has been reported [11] that, with only few exceptions, the elastic moduli of most polycrystalline films have the same strengths as those of their bulk materials. We assume the same behavior of elastic moduli for the thin films tested for fracture. While one can find an abundance of data on the temperature dependence of single-crystal elastic moduli, there exists a scarcity of data on the temperature variation of elastic moduli for polycrystalline materials. Instead, we had to rely on the method developed by Hashin and Shtrikman [12,13] for the calculation of E_f^* and ν_f^* in eqn. (7) for a polycrystalline thin film at temperature θ_f^* corresponding to fracture initiation from the data of single-crystal elastic moduli. The method of Hashin and Shtrikman yields much improved, tighter upper and lower bounds than those obtained by using the approximations of Voigt [14] and Reuss [15]. The elastic moduli of the polycrystalline sample derived from the method of Hashin and Shtrikman are safely estimated to have errors less than 3% for the Young's modulus and less than 1% for the Poisson ratio which varies very slowly with temperature. The single-crystal data over a wide temperature range were taken from the work of Gerlich and Fisher [16] for aluminum and of Chang and Himmel [17] for copper, silver and gold. It turns out that at θ_f^* the Young's moduli of aluminum, copper, silver and gold decrease from their room temperature values by approximately 16%, 14%, 10% and 6% respectively.

The initial thickness d_0 of the film was estimated from Ohm's law

$$R_0 = \rho_0 l_0 d_0 w_0 \tag{8}$$

where ρ_0, l_0, and w_0 are the electrical resistivity, length and width of the film respectively prior to the application of a current pulse. Table 1 lists the results of our experimental data with those values relevant for the calculation of σ_f^* given by eqn. (7). A graphical representation of σ_f^* *vs.* θ_f^* according to eqn. (7) is displayed in Fig. 6, which indicates that, among the high conductivity films of the four different materials considered, the copper film has by far the toughest fracture strength and the gold film exhibits the lowest. The fracture strengths of the silver and aluminum films fall between those of the gold and copper films.

5. Discussion

Both Table 1 and Fig. 6 indicate the very high compressive fracture strength for every specimen tested as predicted by the fracture theory for specimens under biaxial compression. Whether these values are about eight times as high as those under uniaxial tension at the corresponding temperatures remains to be seen. It is also expected that the surface condition of the substrate will affect fracture strength a great deal, because the irregular spots under biaxial compression exerted in the plane of the film act as stress concentrators, thus contributing to a decrease in fracture toughness, while those surface irregularities might enhance a lift-off stress in the direction normal to the plane of the film because of an increased interface area and thus contribute to the better adhesion strength of the film on the substrate. All the fused quartz disks used as substrates are of an optically scratch-free, window grade and not of an extremely fine-surfaced, electronic grade. Investigation of the dependence of fracture strength on the surface condition is left for subsequent work.

TABLE 1. Relevant data for fracture strength and results

Specimen	d_0 (μm)	R_0 (Ω)	R (Ω)	γ (C^{-1})	θ_f^* (C)	E_f^* (GPa)	ν_f^*	$(\alpha_f^* - \alpha_s^*)\theta_f^*$	$-\sigma_f^*$ (GPa)	σ_0^* (MPa)
Al 1	0.195	2.768	5.952	0.0038	300	58.4	0.36	0.0070	0.639	80.0
Al 2	0.190	2.850	5.876	0.0038	276	59.3	0.36	0.0064	0.593	74.1
Al 3	0.201	2.683	5.744	0.0038	296	58.6	0.36	0.0069	0.632	79.0
Ag 1	0.369	0.977	1.894	0.0041	229	64.0	0.39	0.0046	0.483	60.4
Ag 2	0.362	0.997	1.939	0.0041	230	64.0	0.39	0.0046	0.483	60.4
Ag 3	0.348	1.037	1.944	0.0041	213	64.5	0.39	0.0043	0.455	56.9
Ag 4	0.375	0.964	1.774	0.0041	205	64.7	0.39	0.0041	0.435	54.4
Ag 5	0.383	0.941	1.872	0.0041	241	63.6	0.39	0.0048	0.500	62.5
Au 1	0.265	1.808	2.998	0.0040	165	73.2	0.43	0.0024	0.308	38.5
Au 2	0.296	1.616	2.718	0.0040	171	73.0	0.43	0.0025	0.320	40.0
Au 3	0.251	1.910	3.236	0.0040	173	72.9	0.43	0.0025	0.320	40.0
Cu 1	0.879	0.388	0.974	0.0041	371	108.5	0.36	0.0065	1.102	138
Cu 2	0.883	0.386	0.937	0.0041	350	109.5	0.36	0.0061	1.044	131
Cu 3	0.890	0.383	0.968	0.0041	376	108.3	0.36	0.0066	1.117	140
Cu 4	0.848	0.402	1.028	0.0041	383	108.0	0.36	0.0067	1.131	141

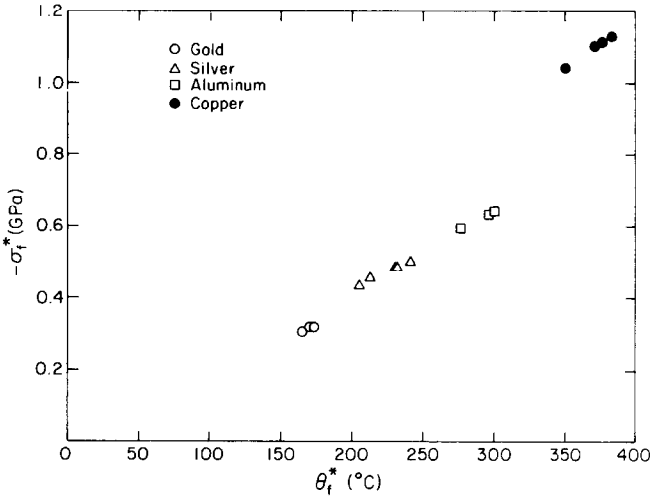

Fig. 6. Fracture strength *vs.* fracture initiation temperature for various thin films.

In the determination of the fracture strength there may exist uncertainties associated with residual stresses induced in the thin film during the deposition process by sputtering. According to the fracture theory, under triaxial loading, the residual stresses either enhance or lower the thermal fracture strength, depending on their distribution and sign. Equation (6) indicates that positive and negative residual σ_{zz} will respectively decrease and increase a thermal stress for initiation of fracture. It is quite likely that, if the sputtering process substantially increased the substrate temperature, the thin film may be under biaxial residual tension which contributes to a higher value of σ_f^*. In addition to the thermally induced residual stresses, intrinsic residual stresses may be introduced in the film because of such factors as a mismatch of atom sizes at the interface, energetic bombardment of particles during the deposition process, microstructures of the film etc. Determination of these residual stresses is quite complicated and outside the scope of the present study. σ_f^* reported here is then a biaxial thermal stress corresponding to the initiation of fracture being obtained under the effect of the residual stresses and should be considered as an *in situ* value which may be of more practical significance in many applications, particularly when the presence of the residual stresses is unavoidable in a specimen. It is otherwise considered as a good approximation to the fracture strength if the residual stresses in the specimen are small or negligible.

The Griffith linear fracture theory [8,9] was used for the calculation of the fracture strength from consideration of the fact that the film fractured in a seemingly brittle manner. The thermal strains $(\alpha_f^* - \alpha_s^*)\theta_f^*$ as listed in Table 1 are somewhat larger than the level which can cause in an unrestrained free specimen yielding and plastic deformation in the planes that contain directions parallel to the z axis. Under the presence of plastic deformation σ_f^* given by eqn. (7) may be interpreted as a reasonable approximation which can be used to make a relative comparison of the fracture toughnesses of various thin film materials. One could simply argue that θ_f^*, the temperature corresponding to the intiation of fracture, would be perhaps a more accurate gauge for comparison of fracture toughness until a better approximation of σ_f^* is found.

The present authors reported in their previous work [3,4] that thermoelastic loading of a thin film by the flow of a high current pulse caused the film to act as a dipolar source of elastic waves that propagated through the substrate. It is here pointed out for reference that fracture of thin films generates a broadband stress wave signal which can be easily detected by both piezoelectric and capacitive transducers and whose bandwidth extends to the audible range.

Acknowledgments

This work has been supported by the Materials Science Center (MSC) at Cornell University. The MSC is funded by the National Science Foundation.

References

1 K. L. Mittal, *Electrocompon. Sci. Technol., 3* (1976) 21.
2 K. L. Mittal, *J. Adhes. Sci. Technol., 1* (1987) 247.
3 K. Y. Kim and W. Sachse, *J. Acoust. Soc. Am., 86* (1989) 875.
4 K. Y. Kim and W. Sachse, in W. Sachse, J. Roget and K. Yamaguchi (eds.) *Acoustic Emission, ASTM Spec. Tech. Publ. 1077*, 1991, p. 67 (ASTM, Philadelphia, PA).
5 L. I. Maissel and M. H. Francombe, *An Introduction to Thin Films*, Gordon and Breach, New York, 1984, Chap. 8.
6 B. J. Aleck, *J. Appl. Mech., 16* (1949) 118.
7 I. A. Blech and A. A. Levi, *J. Appl. Mech., 48* (1981) 442.
8 A. A. Griffith, *Philos. Trans. R. Soc. London, Ser. A, 221* (1920) 163.
9 A. A. Griffith, *Proc. 1st Int. Conf. on Applied Mechanics*, Delft, 1924, p. 55
10 Y. S. Touloukian (ed.) *Thermophysical Properties of High Temperature Solid Materials*, Vol. 1, *Elements*, Macmillan, New York, 1967.
11 R. W. Hoffman, in *Physics of Thin Films*, Vol. 3, Academic Press, New York, 1966, p. 211.
12 Z. Hashin and S. Shtrikman, *J. Mech. Phys. Solids, 10* (1962) 335.
13 Z. Hashin and S. Shtrikman, *J. Mech. Phys. Solids, 10* (1962) 343.
14 W. Voigt, in *Lehrbuch der Krystallphysik*, Teubner, Leipzig, 1928, p. 962.
15 A. Reuss, *Z. Angew. Math. Mech., 9* (1929) 49.
16 D. Gerlich and E. S. Fisher, *J. Phys. Chem. Solids, 30* (1969) 1197.
17 Y. A. Chang and L. Himmel, *J. Appl. Phys., 37* (1966) 3567.